



## Performances of biological aerated filter employing hollow fiber membrane segments of surface-improved poly (sulfone) as biofilm carriers

SHEN Ying-jie<sup>1</sup>, WU Guang-xia<sup>1,\*</sup>, FAN Yao-bo<sup>1</sup>, ZHONG Hui<sup>1</sup>, WU Lin-lin<sup>1</sup>,  
ZHANG Shao-lai<sup>2</sup>, ZHAO Xian-hong<sup>2</sup>, ZHANG Wei-jun<sup>2</sup>

1. Research Center for Eco-Environmental Sciences, Chinese Academy of Sciences, Beijing 100085, China. E-mail: [shen\\_spring@sina.com](mailto:shen_spring@sina.com)

2. Research Institute for Beijing Tongrentang Limited Company, Beijing 100062, China.

Received 8 September 2006; revised 30 October 2006; accepted 18 January 2007

### Abstract

Using the surface of poly (sulfone) hollow fiber membrane segments as grafted layer, the hydrophilic acrylamide chain was grafted on by UV-photoinduced grafting polymerization. The gained improvement of surface wettability for the modified membrane was tested by measuring the contact-angle as well as FTIR spectra. Then correlation between the hydrophilic ability of support material and the biofilm adherence ability was demonstrated by comparing the pollutant removal rates from urban wastewater via two identical lab-scale up-flow biological aerated filters, one employed the surface wettability modified poly (sulfone) hollow fiber membrane segment as biofilm carrier and the other employed unmodified membrane segment as biofilm carrier. The experimental results showed that under the conditions of influent flux 5 L/h, hydraulic retention time 9 h and gas to liquid ratio (G/L) 10:1, the removal rates of chemical oxygen demand (COD) and ammonium nitrogen ( $\text{NH}_4^+\text{-N}$ ) for the modified packing filter and the unmodified packing filter was averaged at 83.64% and 96.25%, respectively, with the former filter being 5%–20% more than the latter. The effluent concentration of COD,  $\text{NH}_4^+\text{-N}$  and turbidity for the modified packing filter was 25.25 mg/L, 2 mg/L and 8 NTU, respectively. Moreover, the ammonium nitrogen removal performance of the filter packing the modified PSF was compared with the other bioreactor packing of an efficient floating medium. The biomass test indicated that the modified membrane matrixes provided better specific adhesion (3310–5653 mg TSS/L support), which gave a mean of 1000 mg TSS/L more than the unmodified membrane did. In addition, the phenomenon of simultaneous denitrification on the inner surface of the support and nitrification on the outer surface was found in this work.

**Key words:** surface modification; UV-photoinduced grafting polymerization; nitrification; denitrification; hollow fiber membrane; biofilm attachment

### Introduction

Among advanced methods of wastewater treatment, treatment with the biological filter, in which biodegradation processes and suspended solid filtration occur simultaneously, that is, can remove not only the chemical oxygen demand (COD) and suspended solids (SS) but also ammonia nitrogen (Cohen-Shoel *et al.*, 2002; Deshusses *et al.*, 1997; Dillon, 1990; Mann *et al.*, 1998; Pujol *et al.*, 1994). The studies on wastewater treatment using biological aerated filters and the development of practical systems have progressed rapidly since the late 1980s (Xie and Wang, 2004; Pujol, 1998; Kazuaki *et al.*, 2003; Nagao, 1990). The selection of a suitable BAF medium is critical in the design and operation of the process to reach the required effluent standards. Nowadays, different types of carriers including sand, expanded clay, poly (propylene),

and polyethylene have been applied widely. However, the biofilm affinity for most medium materials was not good because of their poor surface hydrophilic ability and biocompatibility, which led to low bioactivity and low contaminant removal efficiencies in BAF accordingly.

To take advantage of the membrane production, two kinds of membrane segments having lengths of 5–20 mm were employed as biofilm support in this study. The disposal of main pollutant from urban wastewater, especially to the nitrogen removal was studied using biological aerated filters. To our best knowledge, this is the first time that hollow fiber membrane segments are used as biofilm carriers in this field. The hollow fibers employed in this study were selected due to their availability, the characteristic shape, good permeability of water, outstanding chemical and biological stability, etc. Moreover, the high hydrophilicity of membrane surface make the microorganisms grow and adhere to easily. Nowadays more and more biomedical applications of membrane technology such as membrane-based cell and tissue culture reactors gave good examples for using the optimized biocompatibility of separation

Project supported by the Natural Science Foundation of Beijing (No. 2051002); the Technologies R&D Program of Beijing (No. D0205004000011) and the Hi-Tech Research and Development Program (863) of China (No. 2002AA601220). \*Corresponding author. E-mail: [wgxzhj@yahoo.com.cn](mailto:wgxzhj@yahoo.com.cn).

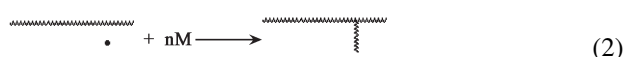
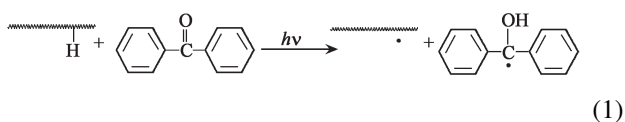
membrane (Ulbricht, 2003).

Furthermore, an important feature of this process is the simultaneous occurrence of nitrification and denitrification. The special shape and the good hydrophilicity for the inner and outer surfaces of these surface-improved hollow fiber membrane segments made it possible for coexistence of anoxic and aerobic bacteria. In this study, the phenomenon of simultaneous nitrification and denitrification was investigated by comparing and analyzing the concentration variations of total nitrogen (TN),  $\text{NH}_4^+\text{-N}$  and nitrate nitrogen ( $\text{NO}_3^-\text{-N}$ ) under different medium height conditions, and the probability of the simultaneous existence for anoxic and aerobic bacteria at the inner and outer surface of the hollow fiber membrane segments could be proved consequently.

## 1 Experiment

### 1.1 Photochemistry surface modification

Using benzophenone (BP) as photo-initiator, acrylamide as graft monomer, the acrylamide chain was grafted on the surface of PSF hollow fiber membrane segments. The experiments were carried out using the photochemical reactor system devised and made in the laboratory of Chinese Academy and Sciences. The photochemical reactor was equipped with a 1000-W high pressure mercury lamp and a quartz glass which permitting UV light penetration. The reactor also had an inlet and outlet vent for nitrogen purging, which was necessary to remove oxygen that could terminate the free radicals formed during photochemical modification. The photografting polymerization process was made by the following procedures: (1) the photo-initiator (benzophenone) was irradiated under UV light; (2) photoreduction by hydrogen abstraction of the ketone from a macromolecular hydrogen donor shown in Equation (1) gave a ketyl radical (which may initiate homopolymerization and a macromolecular free radical that can initiate graft polymerization); (3) as the hydrogen donor was the surface of PSF membranes, surface photografting polymerization was initiated; (4) based on the polymerization Equation (2), the appeared hydrogen atoms form the new partners for the ketone reaction; (5) a secondary photoreduction then occurs, in which the graft polymers chains together.



### 1.2 BAF experimental set-up

A schematic diagram of the experimental set-up is depicted in Fig.1 and Table 1. The lab scale plant consisted of two identical organic glass columns equipped with 9 outlets from the bottom up: A (column) and B (column), each had loading cubage of  $0.66 \text{ m}^3$ . The two up-flow columns were filled with:

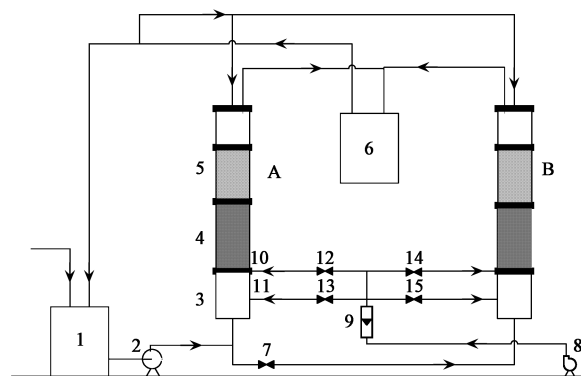


Fig. 1 Lab scale plant process. (1) service flume; (2) constant-flow pump; (3) anaerobic tank; (4) aerobic tank (plentiful DO cell); (5) aerobic (lesser DO cell); (6) discharged water; (7) liquid; (8) air pump; (9) air flowmeter; (10) diffuser tube; (11) diffuser tube for backwashing; (12, 13, 14, 15) air valve.

Table 1 Operational parameters and capacity of the tested units

Hydraulic loading	0.064–1.0 $\text{m}^3/(\text{m}^2 \cdot \text{h})$
Air flow rate	0.32–2.4 $\text{m}^3/(\text{m}^2 \cdot \text{h})$
Hydraulic retention time	1.2–15 h
Bed height	1.2 m
Total capacity	0.044 $\text{m}^3$
Height ratio (aerobic tank/anaerobic tank)	3.3/1.0
Carrier material	Poly (sulfone), modified poly (sulfone)
Carrier length	5–20 mm
Carrier mean diameter	1.5–3 mm
Carrier density	0.78–1.07 $\text{g}/\text{m}^3$
Operational temperature	22–25°C

A: poly (sulfone) hollow fiber membrane segments;

B: surface modified poly (sulfone) hollow fiber membrane segments (surface hydrophilicity improved).

The municipal wastewater and filtered effluent were mixed in a certain ratio as the uniform influent of the two biological aerated filters. The performance of the biofilm carriers was analyzed by comparing the biofilm formation during start-up. The system operated up-flow since the density of membrane segment was  $0.78\text{--}1.07 \text{ g}/\text{m}^3$ , that is, the wastewater was pumped into the columns from the bottom and the effluent came out from the top. Aeration was done evenly on the section of the filter medium. For each filter, the installation heights of two diffuser tubes were 160 mm and 260 mm from the bottom of the filter medium layer. Thus we can use the upper diffuser tube as an aerator for aerobic tank and the bottom one for backwashing of the reactor. In order to avoid filter clogging, backwashing was carried out every 10 d to remove excess biomass.

The aerobic tank also consists of two parts: the dissolved oxygen-enriched cell in which there was plentiful DO, the other cell in which there was comparatively little DO in comparison with the former. At first, the wastewater was pumped into the anaerobic tank (the medium height of 0–240 mm). In this step, denitrification was achieved by mass of denitrobacteria, and the biological oxygen demand ( $\text{BOD}_5$ ) was biodegraded by microorganism using the oxygen produced during the denitrification. It is worthy to be mentioned here that a quantity of SS was retained from

this first step. In the second step, the wastewater entered the aerobic tank (up from the height of 240 mm), BOD<sub>5</sub> was biodegraded further. The conversion of ammonia into nitrate could be accomplished since nitrification occurred at the outer space of hollow fiber membrane segments. Nonetheless, in parallel to the nitrification process, denitrification still occurs here due to the existence of some denitrobacteria in the inner side of the membrane segments wherein some cells containing comparatively little DO. In the process of backwashing, the combination method of "air-shots" from diffuser tube placed at the lower part and water sprinkling from above was used to wash off the sludge on the surface of membrane segments.

### 1.3 Wastewater composition

The feed stream was the mixture of domestic water and the effluent from the treatment plant in accordance with certain ratio. The treated water was collected and analyzed daily, and its main composition was: chemical oxygen demand (COD) within the range of 270–550 mgO<sub>2</sub>/L; biological oxygen demand (BOD<sub>5</sub>) of 50–87 mgO<sub>2</sub>/L; total nitrogen (TN) of 90–120 mg/L; ammonium nitrogen (NH<sub>4</sub><sup>+</sup>-N) of 50–88 mg/L; total phosphorous (TP) ranged between 5–9 mg/L and pH level between 6.2–8.0.

### 1.4 Analytical methods

The surface wettability of PSF hollow fiber membranes that been grafted with acrylamide was characterized by measuring the contact angles. Attenuated total reflection-Fourier transform infrared (ATR/FTIR) spectra of the base and grafted membrane were measured with a Nicolet Avatar 360 FTIR Spectrometer (Thermo Nicolet Corporation). TSS was measured by Weight method.

Standard methods for the examination of water and wastewater were followed, in which, water samples were analyzed for COD, BOD<sub>5</sub>, TN, NH<sub>4</sub><sup>+</sup>-N, NO<sub>3</sub><sup>-</sup>-N, NO<sub>2</sub><sup>-</sup>-N and turbidity. Temperature and pH were measured using Crison GLP 22 pH-meter, dissolved oxygen (DO) was measured with ORIONA+810A PLUS dissolved oxygen measurer. COD was analyzed using the potassium dichromate method. Nessler's reagent colorimetric method was used to measure the concentration of NH<sub>4</sub><sup>+</sup>-N, and the spectrophotometric analysis kits were applied to analyze TN, NO<sub>3</sub><sup>-</sup>-N and NO<sub>2</sub><sup>-</sup>-N.

## 2 Results and discussion

### 2.1 Role in biofilm adherence of membrane segments as carriers

The dissolved oxygen and nutrient substances needed in the synthesis process of microorganism were carried by water in BAF system, so the surface water permeability of support medium materials would, to some extent, influence the biofilm formation on the inner surface of the support mediums. The good diffusivity of water between both surfaces of the employed membrane segments was the influential factor of biofilm attachment on the carrier's surface.

In comparison with other floating medium material, such as polyethylene and polypropylene etc., the PSF membrane material had higher water flux and better water permeability between its inner space and outer space through the membrane pores.

Other than that, the modified PSF membrane segments could provide more ideal living environment for microbes than the unmodified ones because of the improvement of surface hydrophilicity.

### 2.2 Differences in hydrophilic ability and biofilm adherence ability

#### 2.2.1 Comparison of surface hydrophilic ability between modified membrane and unmodified membrane

In this experiment, the surface of poly (sulfone) membranes was modified by UV photo-grafting polymerization process. The surface of the PSF hollow fiber membranes grafted with acrylamide was characterized by water contact angle measurements, since contact angle could be an indicator of surface wettability/hydrophilic ability. If the surface wettability is higher, the contact angle is smaller. We measured the contact angles of the membrane by the sessile drop method using the Contact Angle Device (CAD). The hollow fiber membrane was dissected from its sides, and then was placed on a flat glass surface. After that a drop of distilled water was deposited onto the membrane surface, and the contact angle was measured by screwing the goniometer.

Fig.2 shows a comparison between contact angle of the modified and unmodified PSF hollow fiber membrane under the different condition of UV photo-irradiation time.

It could be seen that contact angles of the unmodified membrane remained at about 70°, whereas those of the modified membrane were at about 48° with irradiation time of 10 min. The decrease of contact angles from 70° (for unmodified membrane) to 48° illustrated the improvement of surface hydrophilic ability. This improvement maybe attributed to the increase of quantity of hydrophilic polymer chains grafting on the surface of membrane segments.

#### 2.2.2 Surface chemical structure analysis of the modified PSF hollow fiber membranes

In order to find the chemical structure of the modified membranes, Attenuated total reflection-Fourier transform infrared (ATR/FTIR) spectra of the base and modified membrane were measured. There was a distinct mer-

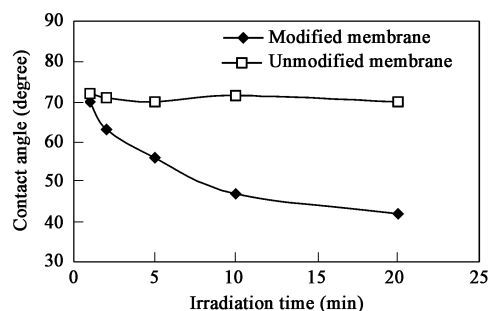


Fig. 2 Contact angle changes of membrane with different irradiation time.

it of adjusting analyzed surface depth in this method. ATR/FTIR spectra of inner surface of modified PSF and unmodified PSF membranes are shown in Fig.3. It could be seen that in case of the modified membrane, a new infrared spectroscopy adsorption was detected at  $1670\text{ cm}^{-1}$  representing C=O stretch peak and abroad band near  $3050\text{--}3100\text{ cm}^{-1}$  represented N-H stretch. These observed differences in the spectra of the modified and unmodified membranes proved that there were polyacrylamides group grafted on the inner surface of PSF membranes.

### 2.2.3 Quantification of biomass attachment on the supports

The microorganisms were fed by using the continuous feed water method. Process liquid was employed to start-up the system and water flow rates were regulated by constant-flow pumps.

During 45 d of operation, the biomass concentrations on the biofilm supports were measured. Because the weight of membrane segment was much heavier than the graft monomer used in their modification, the weight difference between unmodified membrane segment and modified membrane was so little that it could be ignored. Fig.4 illustrates the adhesion of the organisms (quantified as total suspended solids) on each support material at the height of 360 mm (in the aerobic tank) and 160 mm (in the anaerobic tank) from the bottom of the filters media layers throughout the experiment. The results indicated that the modified membrane matrixes provided better specific adhesion on the range of 3310–5653 mg TSS/L support, in comparison with that of 2264–4552 mg TSS/L support for the unmodified membrane.

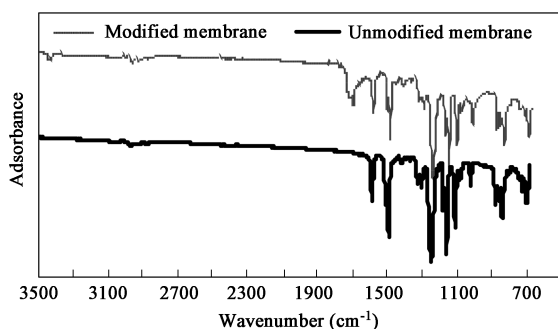


Fig. 3 FTIR spectra of modified membrane.

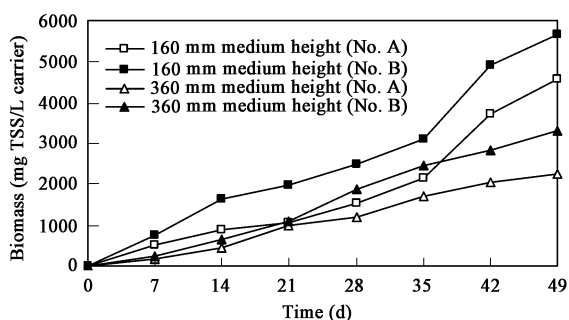


Fig. 4 Variation of biomass adhered to different support material under the different medium height conditions.

Both modified membrane material and unmodified membrane presented higher biomass concentration in the anaerobic tank than in the aerobic tank. The reason was that the feed water firstly flew through the anaerobic tank and thus the concentration of nutrients in the anaerobic tank was higher than that in the aerobic tank.

Although the biomass in column B was greater in number than in column A, there was a little difference in filtration rates between the two columns. It was logically thought that the comparatively good surface water permeability of the modified membrane segments contributed to the fluid flow in the reactor to some extent.

### 2.3 Comparison of pollutant removal rates during start-up

To demonstrate that the surface hydrophilic ability of support materials can lead to different microbial equilibrium which directly affects the reactor's performance and stability, the COD and nitrogen removal of column A and column B were compared; the influences of the surface wettability on the biofilm adherence were studied accordingly.

#### 2.3.1 Comparison of COD removal between column A and column B

As shown in Fig.5, COD removal efficiency between column A and column B were compared. Within the first 15 d, the removal rates of the two columns were low and fluctuate drastically because the bacteria were small in number. The loss of COD would logically be assumed to the adsorption by filter medium. Moreover, the organic compound that was retained by the filter medium increased the surface roughness of the filter medium, and thereby the adsorption was intensified. The abrupt increase in the concentration of COD in influent led to the decrease of removal rates at the day 11.

From the day 17, the removal rates of column B were 7%–20% higher than that of column A, and the color of the carriers' surface in the latter was deeper than that in the former. It was clearly manifested that owing to the high hydrophilic ability of modified membrane segment and the high sorption ability for microorganisms, there were higher biomass and more uniform biofilm distribution in the column B.

#### 2.3.2 Contrast of ammonium nitrogen removal rates between column A, column B and the filter C

It can be observed from Fig.6 that there was scarcely any influence of carriers' hydrophilic ability on the ammonium nitrogen removal within 17 d. This is because nitrifying bacteria had long generation time. The high organic load of the influent would restrain the propagation of nitrifying bacteria to some extent as well. We could see that after 40 d the ammonium nitrogen removal rates of column B approached 90% that was slightly higher than that of column A.

The ammonium nitrogen removal rates of the bioreactor packing of an efficient floating medium (filter C) were described by Xu *et al.* (2003), whose cubage was  $6.0\text{ m} \times$

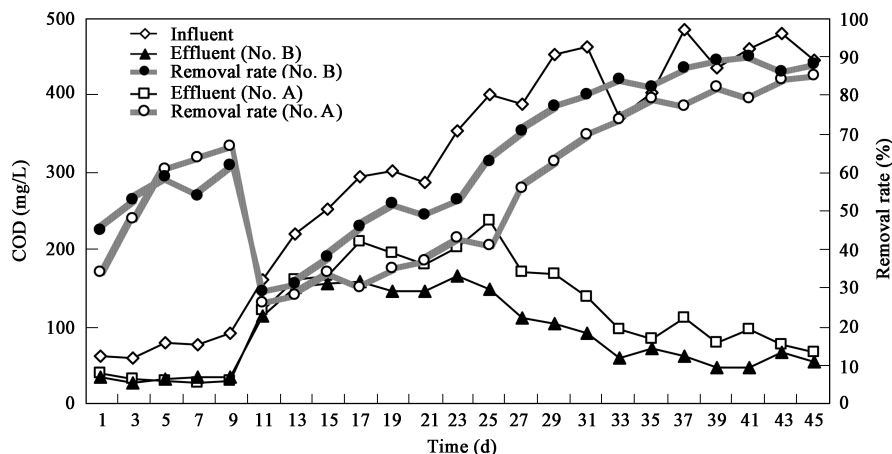


Fig. 5 Effects of COD removal for column A and column B during start-up.

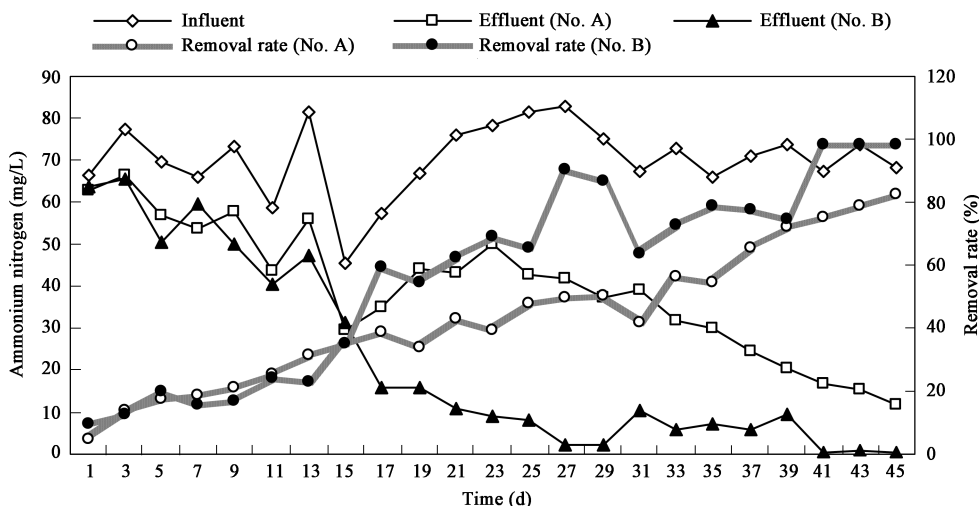


Fig. 6 Effects of ammonium nitrogen removal for column A and column B during start-up.

1.5 m × 9.5 m. The removal rates of filter C achieved 70% after 1 week in start-up process and the maximum removal rate was 77.7% in steady state with the influent flux of 80 m<sup>3</sup>/h, the air flux of 60 m<sup>3</sup>/h and the mean ammonium concentration for influent of 3.05–65 mg/L. Fig.6 shows that although the removal rate of column B did not exceed the 20% during initial stages, 100% removal rate was achieved in steady state with mean ammonia concentration for the influent of 70 mg/L. Calculations of the ammonium removal rates on the basis of the loading acreage for the mediums showed that values of 206 g/(m<sup>2</sup>·d) and 213 g/(m<sup>2</sup>·d) were obtained in case of column B and filter C, respectively. Consequently, a conclusion can be drawn that the modified membrane segments could be used as a

new type of biofilm carriers but the operation condition of biofilm formation should be investigated further.

**2.3.3 Nitrate nitrogen volumetric load and the removal rate in the anaerobic tank**

Denitrification was achieved by mass of denitrobacteria using the organic compounds as organic carbon resource in the anaerobic tank (the medium height of 0–240 mm), as a result, the conversion of NO<sub>3</sub><sup>-</sup>-N into N<sub>2</sub> was accomplished. Table 2 provided the correlation between NO<sub>3</sub><sup>-</sup>-N volumetric load and denitrification rate in anaerobic tank of two columns. The NO<sub>3</sub><sup>-</sup>-N volumetric load was calculated from the influent NO<sub>3</sub><sup>-</sup>-N concentration on the basis of the capacity of the anaerobic tank. Although the NO<sub>3</sub><sup>-</sup>-N volumetric loading of the anaerobic tank varied from

**Table 2 Nitrate nitrogen load and the removal rate in anaerobic tank**

Volumetric load (kg/(m <sup>3</sup> ·d))	Influent NO <sub>3</sub> <sup>-</sup> -N (mg/L)	Effluent (column A) (anaerobic tank) NO <sub>3</sub> <sup>-</sup> -N (mg/L)	Effluent (column B) (anaerobic tank) NO <sub>3</sub> <sup>-</sup> -N (mg/L)	Removal rate (%) (column A)	Removal rate (%) (column B)
0.080	7.4	1.6	1.4	79.7	82.0
0.205	15.8	2.7	2.1	83.1	86.1
0.462	34.3	13.5	10.4	60.6	69.7
0.282	21.0	4.4	3.2	80.0	85.4
0.558	39.5	12.9	8.5	67.4	79.6

0.080 to 0.558 kg/(m<sup>3</sup>·d), the NO<sub>3</sub><sup>-</sup>-N removal rate was maintained above 60% within the loading range. These results demonstrated high denitrification rate of the tested systems.

As it can be seen from Table 2, the removal rate of column B was higher than that of column A under the same nitrate nitrogen volumetric load, which indicated the denitrobacteria attachment on the modified membrane segments were larger in number than that on the unmodified membrane segments.

## 2.4 Nitrogen removal characteristic for filter B

### 2.4.1 Concentrations of ammonium nitrogen, nitrate nitrogen and nitrite nitrogen of column B during start-up

In order to study the nitrogen removal performance further, NH<sub>4</sub><sup>+</sup>-N, NO<sub>2</sub><sup>-</sup>-N and NO<sub>3</sub><sup>-</sup>-N concentrations of column B were obtained to determine the period of time needed to establish a biofilm capable of nitrifying inlet nitrogen to nitrate (Fig.7). Maintaining the NH<sub>4</sub><sup>+</sup>-N concentrations within the range of 50–70 mg/L in feed water, NO<sub>3</sub><sup>-</sup>-N appeared in the outlet water after 11 d. The time needed to produce nitrates was in consistent with that described by Watson *et al.* (1989) who indicated that nitrifying bacteria need 9 d at 25°C to attain chemolithoautotrophic growth and manifest its oxidizing activity. Once the nitrate concentration reached stationary conditions, nitrite concentration nearly disappeared; this result is in accordance with the report by Metcalf (1995) who described that generation time needed for ammonia oxidizers was larger than for nitrite oxidizers; the ammonia oxidation step becomes the rate-limiting step in nitrification.

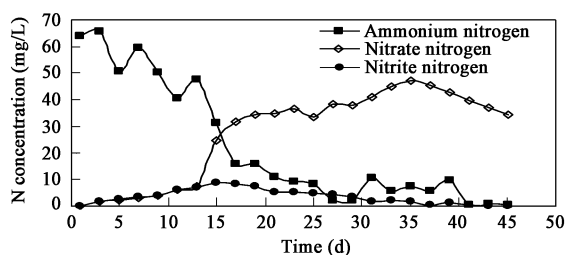


Fig. 7 Contrast among the concentrations of ammonia, nitrate and nitrite in the outlet water during start-up.

On the other hand, nitrogen removal obtained under our experimental conditions was not only due to the nitrification-denitrification process. Obviously, there was also an overall loss of nitrogen, which would logically be assumed to be nitrogen assimilation (Rovel and Mouchet, 1991), ammonia volatilization (Tschui *et al.*, 1993), adsorption on the biofilm due to different electric charges (Nielsen *et al.*, 2002) or through simultaneous nitrification-denitrification in the column.

### 2.4.2 Phenomenon of simultaneous nitrification and denitrification in steady-state

After the start-up, the reactor was operated at different hydraulic loadings starting from 0.064 to 1.0 m<sup>3</sup>/(m<sup>2</sup>·h).

Each hydraulic loading was maintained constant as gas to liquid ratio was increased from 2:1 to 30:1, and steady-state conditions were maintained for 3 weeks. To investigate the effect of the carriers' shape characteristic on the nitrogen removal, the performance of the system under the different medium height conditions were tested while maintaining inlet water flow rate of 5 L/h and the gas to liquid ratio of 10:1. Water samples were collected from the 9 sampling collecting positions placed on the column from the bottom up. Figs.8 and 9 illustrate the experimental results. The concentrations of nitrite nitrogen were less than 1 mg/L in this period, so the effect on nitrite could be ignored. The curves of nitrogen versus the filter height (Fig.8) demonstrated that along with the increase of the medium height the concentrations of TN, NH<sub>4</sub><sup>+</sup>-N and NO<sub>3</sub><sup>-</sup>-N declined from 95–16 mg/L, 55–2.01 mg/L and 34–11.54 mg/L, respectively. The decrease in the amount of NH<sub>4</sub><sup>+</sup>-N and TN indicated the completion of nitrification and denitrification in this reaction system, respectively.

At height range from 0–240 mm, the filter worked as anaerobic tank, where the concentration of dissolved oxygen (DO) was no more than 1 mg/L. At this section, there was little NH<sub>4</sub><sup>+</sup>-N loss since there was little nitrifying bacteria, but there was much loss of nitrate due to the decomposition by mass of denitrifying bacteria. From the height of 240–600 mm, the filter worked as DO-enriched cell in the aerobic tank, where the concentration of DO was 3–5 mg/L. Nitrifying bacteria propagated largely, therefore NH<sub>4</sub><sup>+</sup>-N concentrations declined sharply but NO<sub>3</sub><sup>-</sup>-N concentrations rose there. The phenomenon that there were

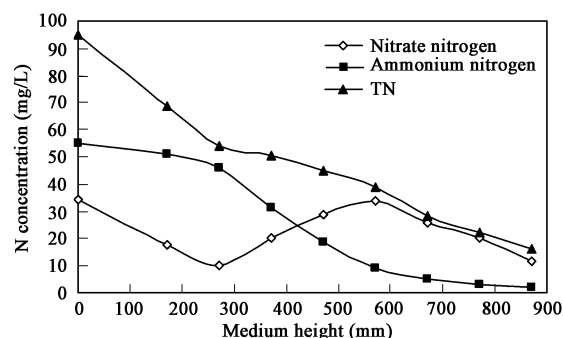


Fig. 8 Nitrogen, ammonia and nitrate concentrations in the outlet water under the different medium height conditions.

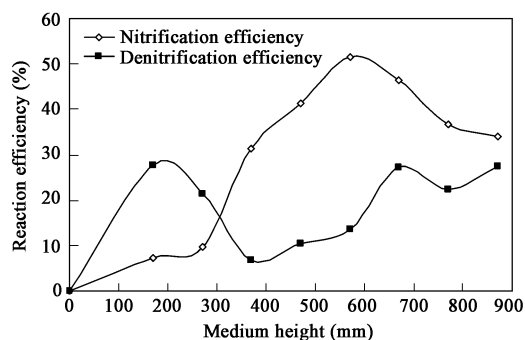


Fig. 9 Profile of nitrification efficiency and denitrification efficiency under the different medium height conditions.

still a few loss of TN proved the occurrence of denitrification. The inner space of membrane segments provided the living space for denitrifying bacteria. Furthermore, there were some sites or zones in the filter wherein DO concentrations were less than 1 mg/L, and accordingly, a few denitrifying bacteria could exist there. Up from the height of 600 mm, the filter worked as a cell in which there was less DO than the DO-enriched cell in the aerobic tank. The DO concentrations in the gaps between carriers were 1–2.6 mg/L and that in the inner surface of some carriers were less than 1 mg/L. Nitrifying bacteria existed on the outer surface of carriers and denitrifying bacteria existed on the inner surface simultaneously, hence, both  $\text{NH}_4^+$ -N and  $\text{NO}_3^-$ -N were biodegraded there.

As a result, the integration of nitrification and denitrification process was possible in different cells in this reactor by measuring and analyzing the concentrations of TN,  $\text{NH}_4^+$ -N and  $\text{NO}_3^-$ -N under the different medium height conditions.

The changes of nitrification efficiency and denitrification efficiency versus the medium height are demonstrated in the Fig.9, The provided results in this figure were calculated according to the nitrogen concentration data of wastewater collected at the different sampling points from the bottom up. It can be seen that the denitrification efficiency of the anaerobic tank was obviously higher than the nitrification efficiency. Furthermore, the nitrification efficiency for the DO-enriched cell in the aerobic tank climbed and leveled off but the denitrification efficiency declined sharply, and the former was higher than the latter. It can also be seen from Fig.9 that although the denitrification efficiency of the other cell increased, it remained lower than the nitrification efficiency. In general, denitrification efficiency was influenced strongly not only by the concentration of DO but also by the amount of organic nutrients.

### 3 Conclusions

After modification, the surface of PSF membrane segments was grafted on hydrophilic monomer, resulting in the improvement of surface wettability.

The surface wettability of the poly (sulfone) hollow fiber membrane segments employed as support materials may influence the biofilm adherence ability during start up.

The biofilm formation on different types of medium materials directly affects the BAF's performance. On comparison with the ammonium nitrogen removal performance of the other bioreactor employing other kind of efficient floating medium, we may come to a conclusion that the modified membrane segments can be used as a new type of biofilm carriers but the biofilm formation operation condition should be investigated further.

The generation time needed for ammonia oxidizers was larger than that for nitrite oxidizers; as a result the ammonia oxidation step becomes the rate-limiting step in nitrification. The nitrogen removal obtained under our experimental conditions was not only due to the nitrification-denitrification process, but there was some nitrogen loss

due to nitrogen assimilation, ammonia volatilization, and absorption on the biofilm due to different electric charges or through simultaneous nitrification-denitrification in the column.

By comparing and analyzing the concentration variations of TN,  $\text{NH}_4^+$ -N and  $\text{NO}_3^-$ -N under different medium height conditions, the phenomenon of simultaneous nitrification and denitrification has been found in this system, and thus the possibility of nitrifying bacteria existing on the outer surface of carriers and denitrifying bacteria existing on the inner surface simultaneously has been proved. Furthermore, the concentration of DO and organic nutrients will influence the nitrification and denitrification efficiency.

### References

- Cohen-Shoel N, Barkay Z, Ilzyer D *et al.*, 2002. Biofiltration of toxic elements by Azolla biomass[J]. *Water Air and Soil Pollution*, 135(1-4): 93–104.
- Deshusses M A, Chen W, Mulchandani A *et al.*, 1997. Innovative bioreactors[J]. *Current Opinion in Biotechnology*, 8(2): 165–168.
- Dillon G R, 1990. A pilot scale evaluation of the biocarbon process for the treatment of settled sewage and for tertiary nitrification of secondary effluent[J]. *Wat Sci Tech*, 22(1/2): 305–316.
- Kazuaki H, Akihiko T, Satoshi T *et al.*, 2003. Simultaneous nitrification and denitrification by controlling vertical and horizontal microenvironment in a membrane-aerated biofilm reactor[J]. *Journal of Biotechnology*, 100: 23–32.
- Mann A *et al.*, 1998. A comparison of floating and sunken media biological aerated filters for nitrification[J]. *Chem Technol Biotechnol*, 72(3): 273–279.
- Metcalf E, 1995. *Wastewater engineering-treatment, disposal and reuse*[M]. Third ed. New York: McGraw-Hill Publishing.
- Nagao H, 1990. Development of rapid filtration equipments for smallscale sewage treatment plant[J]. *Water Waste*, 26(15): 18–22.
- Nielsen P H, 2002. Abundance and phylogenetic affiliation of iron reducers in activated sludge as assessed by fluorescence *in situ* hybridization and microautoradiography[J]. *Applied and Environmental Microbiology*, 68: 4629–4636.
- Pujol R, Hamon M, Kandel X, 1994. Biofilters; flexible, reliable biological reactor[J]. *Wat Sci Tech*, 29(10): 33–38.
- Pujol R, 1998. A key point of nitrification in an upflow biofiltration reaction[J]. *Wat Sci Tech*, 38(3): 43–49.
- Rovel J M, Mouchet P, 1991. *Degrémont water treatment handbook*[M]. Paris : Lavoisier Publishing.
- Tschui M, Boller M, Gujer W *et al.*, 1994. Tertiary nitrification in aerated pilot biofilters[J]. *Wat Sci Tech*, 29(10/11): 53–60.
- Ulbricht Mathias, 2003. Advanced functional polymer membranes[J]. *Journal of Polymers*, 47: 2217–2262.
- Watson S W, Bock E, Harms H *et al.*, 1989. *Bergey's manual of systematic bacteriology*[M]. Ninth ed. Baltimore: William & Wilkins Company.
- Xie W M, Wang Q H, 2004. Upflow biological filtration with floating filter media[J]. *Process Biochemistry*, 39: 765–770.
- Xu B, Xia S Q, Gao T Y *et al.*, 2003. Study on nitrification of the micro-polluted raw water in a suspended packing bioreactor[J]. *Acta Science Circumstantiae*, 23(6): 742–745.